Chemistry & Biology
Article

Rerouting Chlorambucil to Mitochondria Combats Drug Deactivation and Resistance in Cancer Cells

Sonali B. Fonseca,[1,4] Mark P. Pereira,[2,4] Rida Mourtada,[1] Marcela Gronda,[3] Kristin L. Horton,[2] Rose Hurren,[3] Mark D. Minden,[3] Aaron D. Schimmer,[3] and Shana O. Kelley[1,2,*]
[1]Department of Pharmaceutical Sciences, Faculty of Pharmacy
[2]Department of Biochemistry, Faculty of Medicine
University of Toronto, Toronto, ON M5S 1A8, Canada
[3]Princess Margaret Hospital, Ontario Cancer Institute, Campbell Family Cancer Research Institute, Toronto, ON M5G 2M9, Canada
[4]These authors contributed equally to this work
*Correspondence: shana.kelley@utoronto.ca
DOI 10.1016/j.chembiol.2011.02.010

SUMMARY

The difficulty of accessing the mitochondrial matrix has limited the targeting of therapeutics to this organelle. Here, we report, to our knowledge, the first successful delivery of an active DNA alkylating agent—chlorambucil—to mitochondria, and describe unexpected features that result from rerouting this drug within the cell. Mitochondrial targeting of this agent dramatically potentiates its activity, and promotes apoptotic cell death in a variety of cancer cell lines and patient samples. This retention of activity is observed even in cells with resistance to chlorambucil or disabled apoptotic triggering.

INTRODUCTION

The energy-producing capacity of mitochondria (mt) is contingent on the preservation of a barrier limiting the permeation of ions or other small molecules. The highly hydrophobic, densely packed structure of the inner mitochondrial membrane is impenetrable to most molecular species—a property critical for the proton gradient that directs oxidative phosphorylation (Muratovska, et al., 2001). However, the impermeability of this inner membrane impedes the delivery of drug molecules that could impact the other important biological role of mt—apoptotic triggering (Taylor, et al., 2008). Given that apoptotic resistance is observed in many types of cancer cells (Hanahan and Weinberg, 2000), being able to intervene by targeting apoptotic agents to mt could enable the development of new anticancer strategies. In an effort to provide carriers for mitochondrial delivery of bioactive cargo, our group recently developed mitochondria-penetrating peptides (MPPs) that can efficiently traverse both the plasma membrane and mitochondrial membranes with a variety of attached cargos (Horton, et al., 2008; Yousif, et al., 2009). Here, we investigate the impact of mitochondrial delivery of a cargo with clinically relevant anticancer activity, the nitrogen mustard chlorambucil (Cbl). Cbl is a potent alkylating agent that is used to treat leukemia, and its activity is linked to alkylation of the nuclear genome (Begleiter, et al., 1996). We report the rerouting of this agent to the mt and document the unique ability of this organelle-specific drug, mt-Cbl, to evade two commonly observed resistance mechanisms that deactivate cancer therapeutics.

RESULTS AND DISCUSSION

Generation of a Mt-Targeted Form of Cbl and Initial Toxicity Testing

Cbl was selected as an ideal drug for mitochondrial delivery because it exhibits rapid reaction kinetics and does not require cellular activation. In addition, the carboxylic acid moiety provides an ideal functional group for facile attachment to an MPP. To generate mt-Cbl, the drug was coupled to an MPP with the sequence F_xrF_xrF_xr (F_x = cyclohexylalanine, r = d-arginine) (Figure 1A). The peptide sequence was designed based on previous work indicating that the inclusion of cyclohexylalanine units within a sequence introduces sufficient hydrophobicity to allow penetration of the mitochondrial membranes, whereas cationic units drive uptake across the energized barrier enclosing mt (Horton, et al., 2008). Penetration of the peptide into the mitochondrial matrix was confirmed with a biotinylated MPP that could be visualized by immunogold TEM (Figure 1B; see Figure S1A available online). This peptide is comprised entirely of artificial amino acids, which make it resistant to intracellular degradation. The peptide was generated by conventional solid-phase synthesis, and the drug was then attached by coupling to a C-terminal lysine residue. Retention of the alkylation activity (Figure S1B) and DNA-crosslinking activity (Figure S1C) of Cbl in the mitochondrially targeted conjugate were confirmed in vitro.

Initial confirmation of mitochondrial localization for mt-Cbl was obtained by generating a labeled conjugate with the fluorophore thiazole orange (Carreon, et al., 2007) coupled to the N terminus of the peptide. In live HeLa cells, mt-Cbl localization strongly correlated with that of the mt-specific dye MitoTracker, suggesting that Cbl successfully accumulated within the mt (Figure 1C).

The cytotoxicity of mt-Cbl toward HeLa cells was compared to the parent peptide and unconjugated Cbl. Using a cell viability assay, a 100-fold increase in potency was observed with mt-Cbl compared to Cbl (Figure 1D). The parent peptide did not show appreciable toxicity in the concentration range tested, indicating that cell death resulted from the activity of the drug and not the vector.

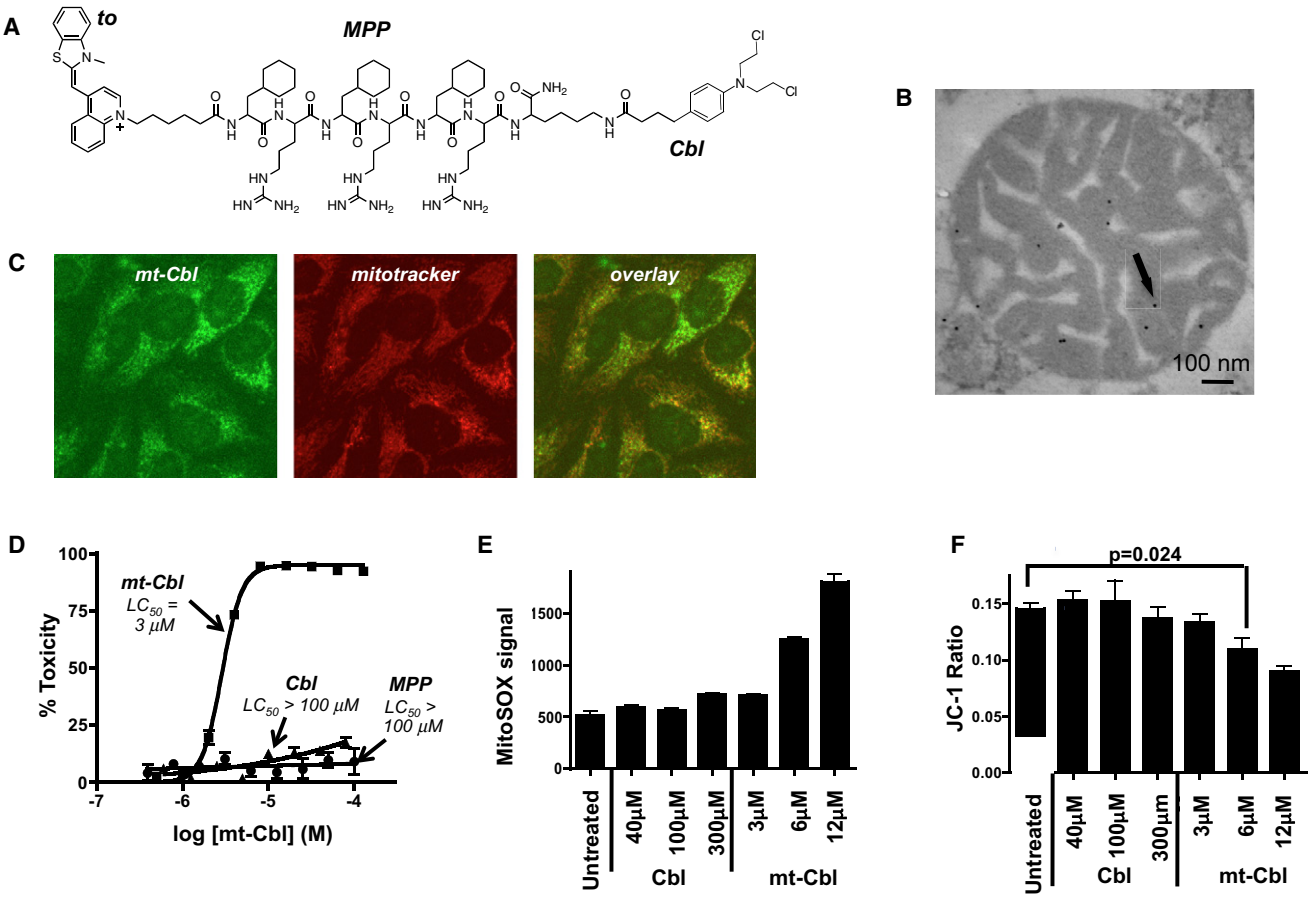

Figure 1. Mitochondrial Localization and Toxicity of mt-Cbl

(A) Structure of fluorescently labeled mt-Cbl conjugate used in studies of mitochondrial drug localization. In all other assays an acetyl group replaced the thiazole orange (*to*) fluorophore on the peptide N terminus. See also Table S1.

(B) Localization of MPP in mitochondrial matrix as observed by immunogold staining and TEM imaging of isolated mt (see Figure S1A for quantitation and controls).

(C) Intracellular localization of *to*-mt-Cbl (green) in live HeLa cells compared with MitoTracker 633 (red).

(D) Toxicity of mt-Cbl toward HeLa cells after 24 hr of incubation. See also Figure S1.

(E) Increased levels of superoxide with mitochondrial targeting of Cbl in HeLa cells. MitoSOX staining and assessment by flow cytometry was consistent with increased superoxide in mt-Cbl treated samples. (F) Mitochondrial delivery of Cbl depolarizes the mitochondrial membrane in HeLa cells. Mitochondrial membrane potential was analyzed by flow cytometry of JC-1 staining. Mean values plotted, n = 3, error bars equal SEM. Student's two-tailed t test used to determine p values.

Cbl is a clinically used therapeutic indicated for the treatment of leukemia (Begleiter, et al., 1996). To evaluate the activity and specificity of mt-Cbl in leukemia cells, we assessed its toxicity in a panel of leukemia cell lines. Similar levels of toxicity were observed. For example, in HL60 cells, mt-Cbl again exhibited an increase in potency compared to Cbl (Table 1), with an EC_{50} of 34 and 6.8 μM for Cbl and mt-Cbl, respectively.

Confirmation of the Mitochondrially Directed Activity of mt-Cbl and Evaluation of the Site of Intracellular Damage

To confirm that cell death arose from reactions occurring in the mt, we looked at two mitochondrial properties: membrane potential and reactive oxygen species (ROS) levels. Mitochondrial DNA lesions have been shown to increase ROS and depolarize this organelle's membrane (Santos, et al., 2003). Both increased superoxide and decreased membrane potential were observed upon mt-Cbl treatment (Figures 1E and 1F). However, Cbl—an agent with activity linked to alkylation of the nuclear genome—did not produce the same phenotypes at statistically significant levels. These data support the hypothesis that mt-Cbl is specifically acting upon mitochondrial targets.

We qualitatively assessed the target of mt-Cbl alkylation within the cell by incubating HeLa cells with the conjugate, allowing alkylation to occur and then fixing the DNA within cells and permeabilizing their membranes. The mt-Cbl conjugate maintained its mitochondrial localization, even upon membrane permeabilization, whereas the MPP control peptide diffused from the mt to the cytoplasm and nucleus upon membrane disruption (Figure S2A). Following fixation and permeabilization, cells were further treated with DNase to fragment the DNA, and this resulted in diffusion of mt-Cbl. These observations qualitatively

Table 1. Summary of EC_{50} Values in Leukemia Cell Line Panel

Cell Line	Cbl EC_{50}	mt-Cbl EC_{50}
OCI-M2	311 ± 24 μM	7.5 ± 1 μM
K562	306 ± 26 μM	8.7 ± 0.4 μM
OCI-LY17	55 ± 7 μM	8.3 ± 1 μM
HL60	34 ± 6 μM	6.8 ± 0.6 μM
U937	34 ± 5 μM	5.9 ± 0.7 μM
OCI-AML2	28 ± 3 μM	6.4 ± 0.4 μM
DAUDI	27 ± 7 μM	9.8 ± 0.8 μM

suggest that mt-Cbl reacts with DNA within mt, and it is this interaction that accounts for retention of mt-Cbl in membrane-permeabilized mt, in contrast to the MPP alone, which lacks the DNA anchor. In addition, isolation of mtDNA after treatment using a biotinylated mt-Cbl indicated that mt-Cbl adducts were present (Figure S2B). This further suggests a covalent attachment of the mt-Cbl to mtDNA.

The alkylation of nuclear versus mitochondrial DNA was quantitatively assessed by comparing the efficiency of PCR amplification of the two genomes. HL60 cells were treated with either Cbl or mt-Cbl, and damage of the nuclear and mitochondrial genomes was assessed independently. A 17.7 kb segment of nuclear DNA at the β-globin gene and an 8.9 kb fragment of mitochondrial DNA were analyzed. Cbl primarily damaged nuclear DNA with very few mitochondrial lesions, whereas mt-Cbl caused a significant reduction of mitochondrial DNA amplification with minimal effect on the nuclear genome (Figure 2). These data suggest that using mt-Cbl specifically targets Cbl's action to mitochondrial DNA.

Interestingly, the levels of damage introduced by Cbl and mt-Cbl in the genomes they target are very similar. Cbl produced 0.42 ± 0.03 lesions per 10 kb in the nuclear genome, and mt-Cbl produced 1.4 ± 0.1 lesions per 10 kb. The similarity in the damage levels observed, despite Cbl treatment at four times its EC_{50} and mt-Cbl treatment at one half its EC_{50}, indicates that mtDNA is more susceptible to alkylation damage.

Differential Cellular Responses to Targeted DNA-Damaging Agents

Having two forms of the same drug targeted to two different organelles provided a unique opportunity to probe how site-specific events within the cell can lead to different responses. We sought to investigate the downstream effects of mitochondrial DNA alkylation relative to those of nuclear DNA alkylation, and to identify the pathways involved in detection of mt-DNA damage and induction of apoptosis. A quantitative real-time PCR array was employed to assess a panel of 84 genes, ten of which have mitochondrial activity (Table S2). These ten genes are known to be involved in DNA damage sensing, repair, apoptosis, and cell-cycle arrest. Genes were considered to be differentially expressed if they showed a ≥4-fold change compared to untreated cells (Figure S3A), and hits were confirmed with three biological replicates using individually synthesized PCR primers.

This analysis revealed that different pathways are activated when nuclear versus mitochondrial DNA alkylation occurs. DDIT3/GADD153 exhibited a 5-fold increase in expression in response to Cbl but no change with mt-Cbl, suggesting that this gene is primarily involved in responding to nuclear DNA damage. Two other genes were upregulated to a greater extent with mt-Cbl relative to Cbl alone: PPP1R15A/GADD34 (4-fold) and GADD45G (15-fold) (Figure 3). p21 was overexpressed in the presence of both mt-Cbl and Cbl. These changes in mRNA levels were confirmed to lead to a corresponding change in protein expression (Figure S3B). Interestingly, none of the genes mentioned above that are known to be mitochondrially targeted were affected.

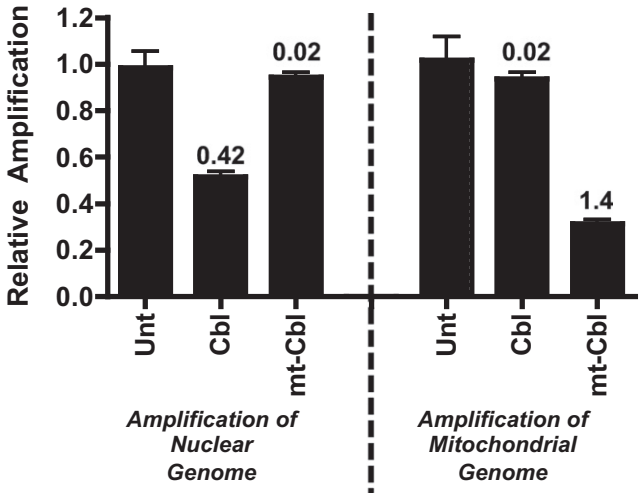

Figure 2. Cbl and mt-Cbl Induce DNA Damage in Different Organelles

Relative amplification of 17.7 kb nuclear and 8.9 kb mitochondrial DNA segments. HL60 cells were treated with Cbl (150 μM) or mt-Cbl (3 μM) for 2 hr prior to PCR analysis. Lesions/10 kb values are included above the graph bars. See also Figure S2.

The Growth Arrest and DNA Damage-inducible (GADD) family of genes are known to be involved in apoptosis and cell-cycle arrest (Smith and Fornace, 1996), and the p21 protein is also known to play an important role in DNA damage sensing. p21 has been shown to interact with GADD45G (Fan, et al., 1999), which can activate p38 or JNK pathways (Lu, et al., 2001). The activation of these pathways was assessed with immunoblotting following treatment with Cbl or mt-Cbl, and interestingly, differential activation was observed, with Cbl activating p38 and mt-Cbl activating JNK (Figure S3C). These results show that different cellular responses are mounted when the same compound is targeted to distinct intracellular sites.

The levels of Ligase III were also investigated in Cbl and mt-Cbl treated cells. This ligase, present in both the nucleus and mt, is the only ligase in the latter organelle and is involved in the repair of most forms of DNA damage (Lakshmipathy and Campbell, 1999). Therefore, in response to mt-Cbl induced damage of the mitochondrial genome, an increase in expression of this gene should be observed. Indeed, this was detected in cells treated with mt-Cbl (Figure 3; Figure S3B).

Activity of mt-Cbl against Primary Human Cells

Having confirmed that we had rerouted Cbl to a new organelle, the mt, and that we observed an increase in potency with

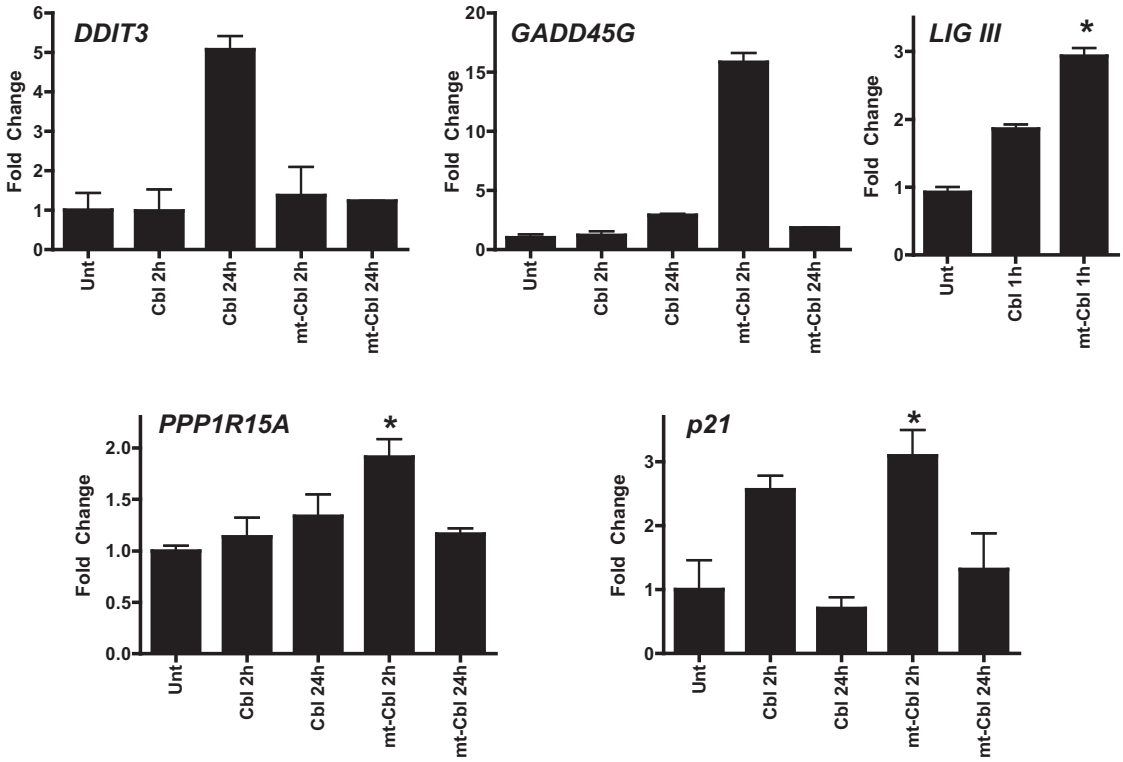

Figure 3. Differing Gene Expression Profiles in Response to DNA Damage by Cbl and mt-Cbl

A qPCR array for genes involved in detecting DNA damage and inducing apoptosis was used to assess RNA expression profiles of HL60 cells treated with LC_{25} doses of Cbl or mt-Cbl for 2 or 24 hr. To assess Ligase III expression, cells were treated with LC_{50} doses of Cbl or mt-Cbl for 1 hr. *MPP change in expression subtracted from mt-Cbl result. Mean values plotted, n = 3, error bars equal SEM. See also Figure S3 and Table S2.

cultured cell lines, we then tested the activity of the drug against primary cancer cells. To determine whether mt-Cbl would show enhanced activity over the parent compound, we assessed toxicity profiles for B cells isolated from patients with chronic lymphocytic leukemia (CLL). To also evaluate the effect of mt-Cbl on normal cells and to examine whether the compound has a clinically useful differential toxicity in normal and malignant cells (i.e., a therapeutic window), the activity of mt-Cbl toward peripheral blood stem cells (PBSCs) and mononuclear cells from normal healthy donors was compared to CLL cells from the peripheral blood of patients. The concentration of mt-Cbl needed to kill cells of patients with CLL was significantly lower than for either population of normal cells, indicating that a therapeutic window exists for the peptide conjugate (Figure 4A). Toxicity of mt-Cbl in primary cells of patients with leukemia was also confirmed through an independent colony-forming assay (Figure S4A). Furthermore, mt-Cbl showed nominal red blood cell-hemolysis levels at the concentrations used in this study (Figure 4A), suggesting a lack of toxicity to these cells at concentrations where leukemic cells were ablated.

To investigate the source of the therapeutic window, we evaluated the cellular uptake of the MPP in the CLL cells, mononuclear cells, and PBSCs. MPP uptake in CLL cells was higher than in normal cells, indicating that higher drug concentrations would be achieved in these cells (Figure 4B). Moreover, a higher relative mitochondrial membrane potential was observed in CLL cells (Figure 4B), suggesting that there would be a greater driving force for mitochondrial accumulation of mt-Cbl in this type of cell. Furthermore, perturbing mitochondrial membrane potential in HL60 cells using the proton ionophore FCCP resulted in a decreased uptake of the MPP, suggesting that mitochondrial membrane potential has an impact on peptide accumulation (Figure S4B). This difference in mitochondrial membrane potential between cancer and normal cells has been widely reported (Davis, et al., 1985), and differential drug toxicity due to this characteristic has also been previously observed, such as in studies with the delocalized lipophilic cations (DLCs) Rhodamine 123 and MKT-077 (Modica-Napolitano and Aprille, 1987, 2001; Modica-Napolitano, et al., 1996). However, here, a drug is being delivered that is not a DLC; and thus, the peptide carrier is providing the necessary specificity. Therefore, MPPs present a general vector for mitochondrial drug delivery with a beneficial therapeutic window.

Activity of mt-Cbl in Drug-Resistant Cells

When the activity of the unmodified drug in a panel of myeloid and lymphoid cell lines (Table 1) was tested, we observed that Cbl had attenuated potency in two cell lines (K562 and OCI-M2). These cells were ~10-fold more resistant than the rest of the cohort (Figure 5B and Table 1). Many cancer cell types are known to increase thresholds for apoptotic induction by altering levels of proapoptotic or antiapoptotic factors, leading to chemotherapeutic resistance. To determine whether the Cbl-resistant cells were generally resistant to apoptosis, we tested the sensitivity of these lines to staurosporine, an Akt inhibitor and inducer of

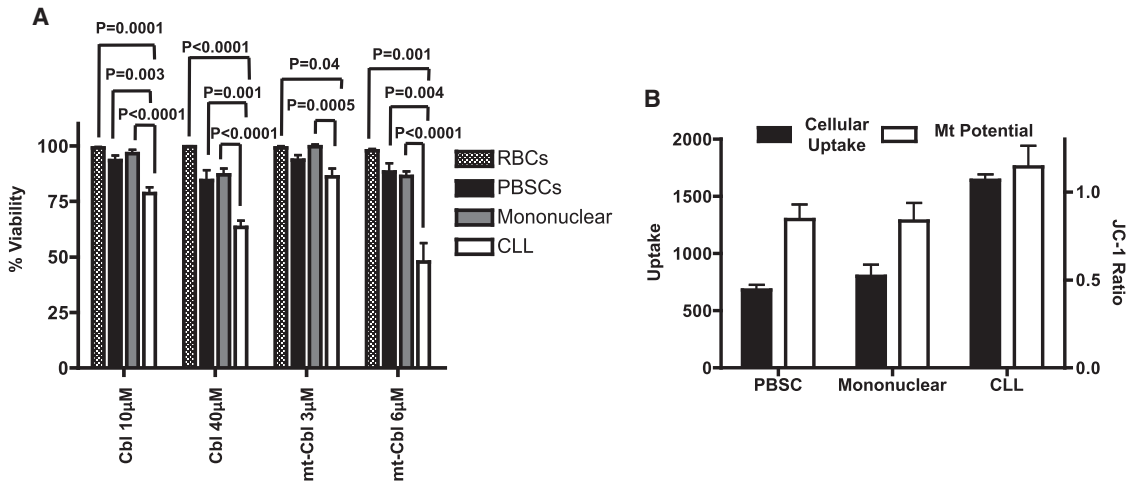

Figure 4. Evaluation of mt-Cbl Activity and Therapeutic Window in primary CLL cells

(A) Cbl and mt-Cbl activity at LC_{25} and LC_{50} in red blood cells (healthy donors), PBSCs (healthy donors), mononuclear cells (healthy donors), and cells of patients with CLL. Both Cbl and mt-Cbl were more selectively toxic to cells of patients with CLL compared to those derived from healthy donors. Percent viability was determined by FACS analysis of Annexin V/SYTOX Red cell staining. Hemolytic activity of RBCs with Cbl and mt-Cbl was found to be minimal at the concentrations used in this experiment. Mean values plotted, n > 5, error bars are SEM. Student's two-tailed t test used to determine p values.

(B) MPP uptake and mitochondrial membrane potential for peripheral blood cells, mononuclear cells, and cells of patients with CLL. Uptake of thiazole orange (*to*)-MPP measured by flow cytometry showed higher levels of peptide uptake in CLL cells. Mitochondrial membrane potential as measured by FACS analysis of JC-1 staining—with a decreasing JC-1 ratio indicative of lower mitochondrial membrane potential—indicated a higher mitochondrial membrane potential for cells of patients with CLL in comparison to PBSCs and mononuclear cells from healthy donors. Mean values plotted, n = 3, error bars equal SEM.

See also Figure S4.

apoptosis. Interestingly, the two Cbl-resistant cell lines showed reduced rates of apoptotic induction (Figure 5C).

Because overexpression of antiapoptotic factors is a common mechanism of apoptotic resistance (Lowe and Lin, 2000; Reed, 1998), we investigated the expression level of the antiapoptotic protein Bcl_{XL}. Bcl_{XL} has been shown previously to be overexpressed in certain cancers, and its antiapoptotic activity is thought to contribute to drug resistance (Minn, et al., 1995). Indeed, in these two Cbl-resistant lines, we observed a much higher level of Bcl_{XL} than in the sensitive lines (Figure 5C). This suggests that Bcl_{XL} overexpression, and the resulting suppression of apoptosis, may underlie the resistance to Cbl. In contrast to Cbl, when the activity of mt-Cbl was tested in this panel using a cell viability assay, comparable toxicity was observed in all lines tested (Figure 5A). Testing toxicity in a secondary assay (induction of apoptosis, Figures 5A and 5B inset), at the EC_{50} concentrations determined from the cell viability assay, showed comparable levels of toxicity (approximately 35% toxicity). In addition the mechanism of cell death for Cbl and mt-Cbl appeared similar, with early apoptotic cells apparent by flow cytometry (inset, Figures 5A and 5B). The fact that the mt-Cbl conjugate still exhibits high levels of cytotoxicity in these apoptosis-resistant cell lines indicates that the delivery of a toxic drug to mt represents an effective means to overcome mechanisms commonly employed by cancer cells to resist the action of cytotoxic drugs. Mitochondrially localized Bcl_{XL} is a component of a pathway that commonly detects apoptotic stimuli from sites outside the mt. Targeting Cbl into the mt to induce toxicity within this organelle might allow the cell to overcome or bypass Bcl_{XL} overexpression and initiate the apoptotic pathway.

Another major form of drug resistance in cancer cells results from the overexpression of enzymes or other factors that facilitate chemical deactivation of pharmacophores. For Cbl, inactivation via glutathione modification is a common mechanism of resistance. Addition of the glutathione tripeptide to Cbl, a reaction catalyzed by glutathione S-transferase (GST), not only results in the inactivation of Cbl (Yang, et al., 1992), but it also promotes efflux from the cell by pumps that recognize glutathione-modified xenobiotics (Barnouin, et al., 1998). In order to analyze whether mt-Cbl would be able to evade drug resistance arising from this type of chemical inactivation, we tested the activity of this conjugate in a Cbl-resistant ovarian cancer cell line known to overexpress the cytoplasmic GST-μ isoform (Horton, et al., 1999). Using the Annexin-V apoptosis assay, we observed that Cbl was able to induce cell death in the wild-type cell line, but in the Cbl-resistant line, toxicity was insignificant, even at 100 μM (Figure 5D). Interestingly, mt-Cbl was able to induce cell death at a much lower concentration (9 μM); this value was comparable in both the wild-type and resistant line. This finding was also confirmed through an independent cell viability assay (Figure S5). Conjugation of the MPP to Cbl, and the subsequent mitochondrial sequestration, appears to limit modification and inactivation by the cytoplasmic GST-μ. The comparable toxicity observed in the wild-type and Cbl-resistant lines supports the notion that targeting and sequestering drugs to the mt also allows for evasion of a chemical mechanism of drug resistance. Given that Cbl resistance has been detected in patients with leukemia (Pepper, et al., 1999), the ability to evade resistance with mitochondrial drug delivery may have clinical relevance.

SIGNIFICANCE

We have demonstrated the advantages of targeting the mitochondria of cancer cells to combat drug resistance

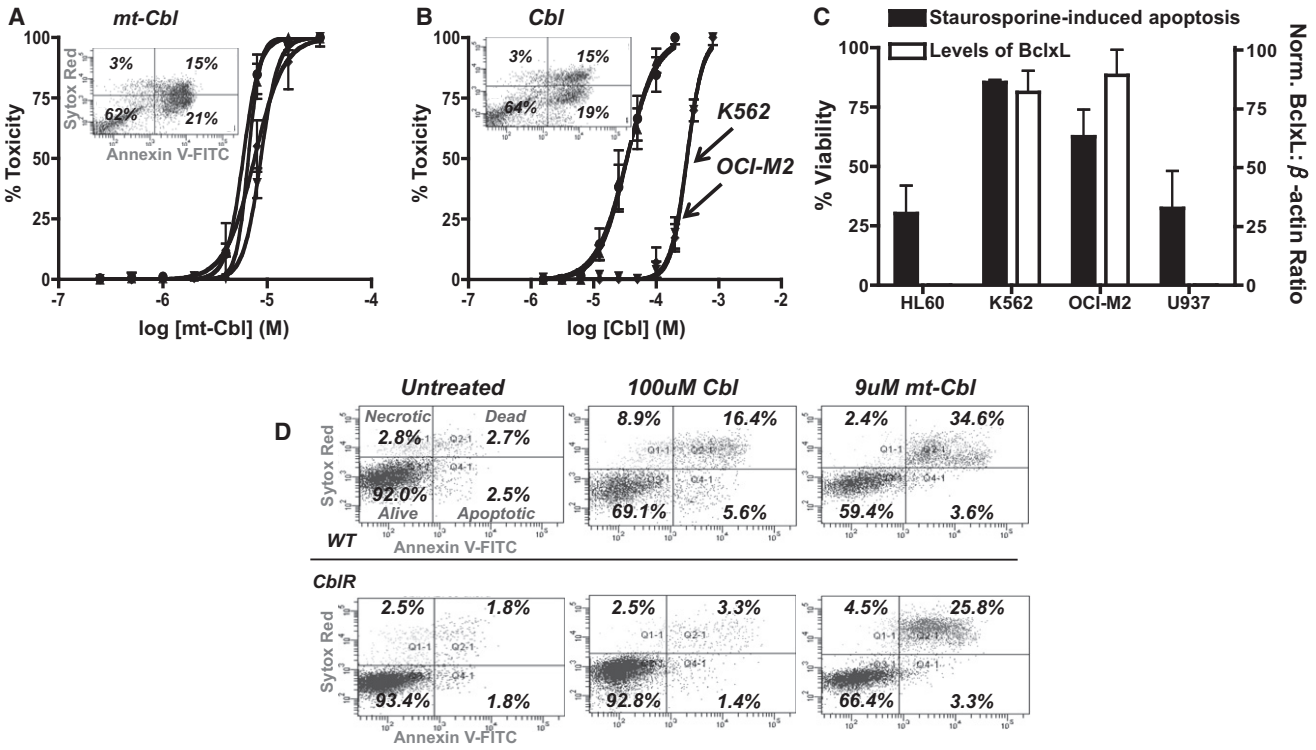

Figure 5. Toxicity of mt-Cbl in Cell Lines Exhibiting Drug Resistance and Apoptotic Resistance

(A) Toxicity of mt-Cbl toward a panel of leukemia cell lines (OCI-M2, K562, HL60, and U937). Mean values plotted, n > 3, error bars are SEM. Inset shows FACS analysis of HL60 Annexin V-FITC (A-FITC)/SYTOX Red (SR) cell staining after treatment with 6 μM mt-Cbl. Indicated are the percentages of population in each quadrant (A-FITC-/SR-, alive; FITC+/SR-, apoptotic; A-FITC-/SR+, necrotic; A-FITC+/SR+, dead).

(B) Toxicity of Cbl with leukemia cell lines showed two distinct populations, with HL60 and U937 being sensitive to Cbl and K562 and OCI-M2 being resistant to Cbl. Inset is the same as (A) but with 34 μM Cbl.

(C) Apoptotic resistance in Cbl-resistant cell lines. Response of leukemia cell lines to staurosporine as measured by FACS analysis of Annexin V-/SYTOX Red-stained cells (black bars). Graphed are percent viable cells. Staurosporine treatment induced less cell death in the K562 and OCI-M2 cell lines compared to HL60 and U937. K562 and OCI-M2 cell lines show higher levels of Bcl-$_{xL}$ expression (white bars). Protein levels were determined by western blot analysis of whole-cell lysates.

(D) Toxicity of mt-Cbl in WT or Cbl-resistant cells (CblR). Cells were treated as in (A). Cbl alone did not show an increase in the apoptotic cell population in CblR; however, an apoptotic response with mt-Cbl treatment was observed for both WT and CblR cell lines. See also Figure S5.

and show that mitochondrial delivery of Cbl results in a significant gain of potency. Importantly, even though the MPP directs Cbl to a novel target—the mitochondrial genome—a therapeutic window was maintained due to differential membrane potentials between CLL cells and normal cells. These studies also illustrate that mitochondrial compartmentalization of Cbl allows for evasion of drug resistance both through biochemical mechanisms like perturbations in the apoptotic pathway, and chemical mechanisms like drug inactivation. Therefore, mitochondrial delivery as a means of "repurposing" FDA-approved drugs currently used in the clinic appears to be a worthwhile strategy to pursue in the development of new anticancer agents.

EXPERIMENTAL PROCEDURES

Peptide and Drug Conjugate Synthesis and Characterization

Solid-phase synthesis was performed on Rink amide MBHA resin (0.7 mmol/g, 100–200 mesh) (NovaBiochem) using a Prelude Protein Technologies peptide synthesizer as described previously (Horton and Kelley, 2009). Peptides were synthesized on a 25 or 50 μmol scale. Thiazole orange was synthesized as described previously (Carreon, et al., 2007) and coupled to peptides using HBTU (4 eq; Protein Technologies, Tucson, Arizona, HBTU = *O*-(benzotriazol-l-yl)-*N,N,N',N'*-tetramethyl-uronium hexafluoro-phosphate), and DIPEA (8 eq; Sigma-Aldrich, St. Louis, DIPEA = *N,N*-diisopropylethylamine) in *N,N*-dimethyl formamide (DMF) overnight. Cbl (Sigma-Aldrich) was coupled to peptides using HBTU (4 eq) and DIPEA (4 eq) in DMF. The N terminus of unlabeled peptides was capped using acetic anhydride, pyridine, and dichloromethane (DCM) (1:5:10; Sigma-Aldrich). Peptides were deprotected and cleaved from the resin using trifluoroacetic acid (TFA):triisopropylsilane:H_2O (95:2.5:2.5) and precipitated in cold ether. All peptides were purified to >95% purity by RP-HPLC on a C18 column with a H_2O/MeCN gradient in 0.1% TFA, and identity was confirmed by electrospray ionization mass spectroscopy. Peptides containing Cbl were immediately flash frozen in liquid nitrogen post-purification and lyophilized to dryness. Thiazole orange-labeled peptides were quantified at 500 nm using an extinction coefficient of 63,000 M^{-1} cm^{-1} (Horton and Kelley, 2009). Cbl-conjugated peptides were quantified at 258 nm using the Cbl extinction coefficient of 15,200 M^{-1} cm^{-1}. Unlabeled peptides were quantified using a BCA assay (Pierce, Rockford, Illinois).

Cell Culture

HeLa cells were cultured in MEM alpha (Invitrogen, Carlsbad, California) supplemented with 10% (v/v) FBS at 37°C with 5% CO_2. U937 cells were cultured in RPMI 1640 plus 10% FBS, and Iscove's modified Dulbecco's media plus

10% FBS was used for OCI-AML2, HL60, K562, OCI-M2, OCI-LY17, and Daudi. A2780 wild-type and Cbl-resistant lines were cultured in RPMI 1640 plus 10% FBS in a humidified atmosphere at 37°C with 5% CO_2. The Cbl-resistant line was treated with 100 μM Cbl once a week for 1 hr to maintain resistance.

Confocal Microscopy—Live Cells

Cells were seeded in 8-well μ-slides (iBidi, Germany) at a density of 25,000 cells per well 1 day prior to experiments. Peptide incubations (5 μM) were performed for the indicated times in OPTI-MEM (Invitrogen). Where stated, MitoTracker 633 (Invitrogen) was added for the last 20 min of the incubation. Cells were then washed twice and imaged using an inverted Zeiss LSM 510 confocal microscope.

Confocal Microscopy—Fixed Cells

HeLa cells were plated as above and treated with 5 μM peptide in MEM alpha without phenol red (Invitrogen) for 5 min at 37°C with 5% CO_2. Peptide solutions were then removed and replaced with fresh media for 25 min at 37°C with 5% CO_2. Cells were washed twice with PBS and incubated with acetone for 10 min at −20°C. Cells were again washed twice with PBS, incubated with 0.1% Triton X-100 for 5 min at 4°C, washed with PBS, and imaged as above. Where stated, cells were incubated with 10 U DNase in 1× DNase buffer for 2 hr at 37°C prior to imaging.

Immunogold/TEM Analysis of Peptide Localization

mt were isolated from fresh mouse liver as previously described (Frezza, et al., 2007). Functionality was confirmed using respirometry. The isolated organelles were used only when the levels of oxygen consumption in state III respiration (presence of ADP) were >4-fold greater than in state II respiration, indicating well-coupled mt. Mitochondrial protein concentration was determined by BCA assay (Sigma-Aldrich). mt were diluted to 0.5 mg/ml in PBS and incubated for 20 min at 25°C with biotin-$F_xrF_xrF_xr$. Cold PBS was added, and mt were pelleted by centrifugation. The pellet was fixed in 1% glutaraldehyde in PBS for 90 min at room temperature, washed with PBS, and then fixed with 1% osmium tetroxide for 2 hr at 4°C. The pellets were dehydrated using graded ethanol, followed by stepwise infiltration with propylene oxide and Epon-Araldite resin. The pellets were cured in resin for 48 hr at 60°C . The blocks were sectioned to 60 nm, and the sections adhered to nickel grids for 30 min at 60°C. The grids were floated on saturated aqueous sodium metaperiodate for 1 hr at room temperature, washed, then blocked with 1% BSA, and labeled with Anti-biotin (Jackson Immunolabs), followed by Protein A-gold (Aurion; 10 nm). The grids were rinsed with water and stained with 2% uranyl acetate for 5 min. To quantitate gold labeling, 200 gold particles (for more densely labeled samples) or 400 mt (for less densely labeled samples) were counted for each counting event. A minimum of three counting events was performed per sample. Counting was performed over different sections.

Analysis of Mitochondrial Superoxide Levels

HeLa cells were plated at 50,000 per well of a 24-well plate 24 hr prior to experiment and treated with Cbl or mt-Cbl in OPTI-MEM (Invitrogen) for 1 hr. Media were removed, and cells were incubated with MitoSOX (Invitrogen) according to manufacturer's instructions. Cells were washed with PBS, trypsinized, and analyzed via flow cytometry with FACSCanto (BD, Franklin Lakes, New Jersey).

Mitochondrial Membrane Potential

HeLa cells were seeded at 50,000 cells per well 24 hr prior to experiment. Samples from patients with CLL, PBSCs, and healthy donor B cells were seeded at 200,000 cells per well in triplicate in a 24-well plate in Iscove's media. Cells were then incubated with 2 μM of 5,5′,6,6′-tetrachloro-1,1′,3,3′-tetraethylbenzimidazolylcarbocyanine iodide (JC-1; Invitrogen) for 20 min at 37°C. Each sample was then washed twice with 1 ml PBS and resuspended in 300 μl PBS prior to being read on a BD FACSCanto. Samples were excited at 488 nm, and emission was collected at 526 nm (green) and 595 nm (red). To obtain the mitochondrial membrane potential (red/green), emission from the red channel was divided by emission from the green channel. For membrane depolarization studies, HeLa cells were treated with Cbl or mt-Cbl for 1 hr in OPTI-MEM (Invitrogen) prior to incubation with JC-1. Cells were washed with PBS, trypsinized, and analyzed as above.

Analysis of Toxicity

HeLa cells were seeded in 96-well flat-bottom tissue culture plates (Starstedt, Germany) at a density of 12,000 cells per well. Leukemic cell lines (K562, OCI-M2, U937, HL60, OCI-AML2, OCI-LY17, Daudi) were seeded in 96-well flat-bottom plates (Greiner Bio-One, Germany) at a density of 50,000 cells per well. A2780 wild-type and A2780 Cbl-resistant cells were plated in 96-well flat-bottom tissue culture plates (Starstedt) at 25,000 cells per well. The culture media were removed, and cells were washed. Peptide incubations were conducted in cell-appropriate media; HeLa cell incubations were conducted in OPTI-MEM media. Cellular viability was analyzed after an overnight incubation at 37°C with 5% CO_2 using the CCK-8 viability dye (Dojindo, Rockville, Maryland) at an absorbance of 450 nm. Statistical analysis was done using GraphPad Prism Software (GraphPad, La Jolla, California).

Colorimetric Alkylation Assay

Alkylation was tested using 4-(4-Nitrobenzyl)pyridine (4-NBP) (Thomas, et al., 1992). Briefly, compound (200–450 μM) was incubated with 4-NBP (0.7% w/vol) in a buffer containing 85 mM triethanolamine (pH 7.2) and 43% acetone. Reactions were incubated at 37°C for 30–120 min. Reactions were terminated by freezing in a dry ice/ethanol bath. To develop samples, 100 μl ethyl acetate and 25 μl 5N NaOH were added followed by vortexing. Absorbance of organic ethyl acetate was read at 540 nm.

Crosslinking of Isolated DNA

Crosslinking of isolated pBR322 DNA was determined from a modification of a published method (Sunters, et al., 1992). Briefly, pBR322 DNA was incubated with compounds at concentrations and times indicated in 25 mM triethanolamine (pH 7.2) and 1 mM EDTA. Reactions were terminated by the addition of 50 mM EDTA and 150 μg/ml excess short oligonucleotide DNA. Samples were denatured at 95°C in denaturation buffer (30% DMSO, 1 mM EDTA, bromophenol blue, xylene cyanol, and 0.4% SDS) for 3 min and flash frozen in a dry ice/ethanol bath. Electrophoresis was carried out in 0.8% agarose in TAE buffer and stained post-run with ethidium bromide.

Quantitative Real-Time PCR

Six hundred thousand HL60 cells were incubated in Iscove's media (Invitrogen) with Cbl, mt-Cbl, or MPP at the LC_{25} dose (17, 3, and 3 μM, respectively) for either 2 or 24 hr as indicated. For Lig3, cells were incubated at an LC_{50} dose (34, 6, and 6 μM, respectively) for 1 hr. RNA was then isolated using the RNeasy Mini-Kit (QIAGEN, Hilden, Germany) according to the manufacturer's instructions. RNA was quantified on a NanoDrop, and 1 μg was converted to cDNA using the RT^2 First Strand Kit (SA Biosciences, Frederick, Maryland). qPCR was then performed using the Human DNA Damage Signaling Pathway PCR Array (PAHS-029; SA Biosciences) or with selected primers purchased from SA Biosciences according to manufacturer's instructions. Data analysis was performed using the web-based software provided by SA Biosciences. Lig3, p21, and GAPDH primers were designed independently: LIG3, forward GAAATGAAGCGAGTCACAAAAGC and reverse GTACCCTTCACATCCTTCAGC; p21, forward CCTCATCCCGTGTTCTCCTTT and reverse GTACCACCCAGCGGACAAGT; and GAPDH, forward CAACGGATTTGGTCGTATTGG and reverse GCAACAATATCCACTTTACCAGAGTTAA. All other steps were performed in an analogous manner to the method described above. Genes showing ≥4-fold change in expression levels compared to control cells were considered hits, as recommended by the SA Biosciences' manufacturer. All hits were confirmed with three biological replicates using primers purchased from SA Biosciences.

Determination of DNA Lesion Frequency by Quantitative PCR

A total of 5 × 10^6 HL60 cells were treated with Cbl (150 μM) or mt-Cbl (3 μM) for 2 hr. DNA was isolated from frozen cell pellets with the QIAGEN Genomic Tip and Genomic DNA Buffer Set Kit (QIAGEN) and quantified using the PicoGreen dye (Invitrogen). Quantitative amplification of the 8.9 kb mitochondrial segment and the 17.7 kb β-globin target sequence was performed using the GeneAmp XL PCR kit (Perkin-Elmer) as described previously (Santos, et al., 2006). Lesion frequency at a given dose, D, was calculated

as $D = -\ln A_D/A_C$, where A_D is the amplification at the dose, and A_C is the level of amplification in nondamaged controls.

mt-Cbl Labeling of mtDNA

Biotin-labeled mt-Cbl peptide (Biotin-mt-Cbl) was synthesized as previously described using Fmoc-Lys(Biotin)-Rink Amide resin (AnaSpec, Inc., Fremont, California). HL-60 cells (25 million cells) were incubated with the compound (0, 1.5 μM) for 30 min, after which the cells were collected. The cells were then washed with ice-cold PBS, and their mt were isolated using Mitochondrial Isolation Kit for Mammalian Cells (Thermo Scientific, Rockford, Illinois). The mtDNA was then extracted from the mitochondrial pellets using AllPrep DNA/RNA Mini Kit (QIAGEN). DNA concentration was measured using a NanoDrop 1000 Spectrophotometer (Thermo Scientific) and then normalized (10 ng/μl). After this, a nitrocellulose membrane was spotted with untreated and treated DNA and UV crosslinked using UV Stratalinker 1800 (Stratagene, La Jolla, California) The membrane was blocked with 5% BSA-TBST for 1 hr at room temperature and then probed with streptavidin-HRP (Sigma-Aldrich) in 5% BSA-TBST (1:5000) at 4°C overnight. Then the membrane was washed and visualized with chemiluminescence detection (GE Amersham, Baie D'Urfe).

Annexin-V Apoptosis Assay

Leukemic cell lines (K562, OCI-M2, U937, HL60) were seeded at 200,000 cells per well of a 24-well plate (Greiner Bio-One). A2780 wild-type and Cbl-resistant cells were plated in 24-well plate at a density of 75,000 cells per well (BD). Healthy donor mononuclear cells were obtained by Ficoll separation from peripheral blood. Samples from patients with CLL, PBSCs, and healthy donor mononuclear cells were plated at 200,000 per well (Greiner Bio-One). Cells were incubated in triplicate with peptides at concentrations indicated in cell-appropriate media. Following overnight incubation at 37°C with 5% CO_2, cells were stained with Annexin V-FITC (BD PharMingen, Franklin Lakes, New Jersey) and SYTOX Red (Invitrogen) according to manufacturer's instructions. Flow cytometry was performed using a FACSCanto (BD). Apoptotic induction by staurosporine was accomplished by addition of 3 μM staurosporine (Sigma-Aldrich) with an overnight incubation.

Colony-Forming Assay

To assess clonogenic growth, primary AML cells (4×10^5/ml) were treated with mt-Cbl in Iscove's media for 2 hr. After treatment, cells were washed, and 10^5 cells/ml were plated by equal volume in duplicate in MethoCult GF H4434 medium (StemCell Technologies, Vancouver, British Columbia, Canada) containing 1% methylcellulose in IMDM, 30% FCS, 1% bovine serum albumin, 3 U/ml of recombinant human erythropoietin, 10^{-4} M of 2-mercaptoethanol, 2 mM of L-glutamine, 50 ng/ml of recombinant human stem cell factor, 10 ng/ml of GM-CSF, and 10 ng/ml of rh IL-3. Seven days after plating, the number of colonies containing ten or more cells was counted as previously described (Buick, et al., 1977).

Western Blots

Leukemia cells were cultured as above and were washed twice with PBS prior to lysis in either Ripa Buffer or 10 mM Tris, 200 mM NaCl, 1 mM EDTA (pH 7.4), 1 mM PMSF, 0.5% NP-40, 1% Triton X-100, 1× Protease Inhibitor Cocktail (BioShop, Burlington, Ontario, Canada) at 4°C, 30 min. Cells were then centrifuged at 1200 rcf, 4°C, 5 min, and protein levels were quantified using bicinchoninic acid (BCA) assay (Pierce). Fifteen to 50 μg of total protein was diluted in 8× sample buffer and heated to 42°C for 5 min prior to loading on 10% or 15% gel. Gels were run at 100 V for 1 hr, and then proteins were transferred onto nitrocellulose or PVDF membranes at 100 V for 1 hr. Membranes were blocked with 5% skim milk or 5% BSA for 1 hr and then probed with primary antibody according to manufacturer's instructions (1:500 Bcl_{XL} antibody [Abcam, Cambridge, Massachusetts], 1:2000 β-actin antibody [Abcam], 1:1000 phospho JNK [Abcam], 1:1000 phospho p38 [Abcam], 1:1000 GADD45G [Santa Cruz Biotechnology, Santa Cruz, California], 1:1000 PPP1R15A [Santa Cruz Biotechnology], 1:1000 DNA Ligase III [Santa Cruz Biotechnology], 1:1000 p21 [Santa Cruz Biotechnology], and 1:1000 DDIT3 [Cell Signaling Technology, Beverly, Massachusetts]). Membranes were then washed and incubated with 1:5000 donkey anti-mouse or goat anti-rabbit IgG-HRP secondary antibody for 1 hr prior to ECL chemiluminescence detection (GE Amersham).

Collection of Patient Samples

Peripheral blood cells from normal individuals and patients with CLL were collected following written informed consent according to a research ethics board (REB) approved protocol. Mononuclear cells were isolated by Ficoll-Hypaque centrifugation. The cells were either used fresh or stored in a viable state at −150°C in 10% DMSO, 40% FBS, and alpha medium. PBSCs were excess filgrastim-mobilized cells obtained from stem cell transplant donors obtained according to an REB approved protocol.

Hemolysis Assay

Red blood cells obtained during Ficoll separation of healthy donor peripheral blood were used for this assay. Cells were washed with PBS until the supernatant was clear. Peptide solutions were made in Iscove's media, and a 1:2 dilution was made across a 96-well plate. To each well, 2 μl of red blood cells was added, mixed, and then incubated for 1 hr at 37°C with 5% CO_2. For 100% lysis, 0.1% Triton X-100 was added to three wells, and for 0% lysis, cells from three wells without peptide were used. Plates were spun at 1000 × g for 10 min, and 50 μl of supernatant was then transferred to a new plate, mixed with 50 μl of PBS, and read at 415 nm to assess for hemolysis.

Peptide Uptake Evaluation

Samples from patients with CLL, PBSCs, and healthy donor B cells were seeded at 200,000 cells per well in triplicate in a 24-well plate in Iscove's media. To determine FCCP effects, cells were pretreated for 15 min with 10 μM FCCP. Cells were then incubated with 2 or 5 μM thiazole orange-labeled peptide for 15 min, washed with PBS, and analyzed on FACSCanto (BD) to determine relative intracellular peptide concentrations.

SUPPLEMENTAL INFORMATION

Supplemental Information includes five figures and two tables and can be found with this article online at doi:10.1016/j.chembiol.2011.02.010.

ACKNOWLEDGMENTS

We gratefully acknowledge the Ontario Institute for Cancer Research (M.D.M.), the Canadian Foundation for Innovation (S.O.K.), and the Terry Fox Foundation Strategic Training Initiative for Excellence in Radiation Research for the 21st Century (M.P.P., R.M.). A.D.S. is a Leukemia and Lymphoma Society Scholar in Clinical Research. Funding for S.B.F. was provided by the NSERC Canada Graduate Scholarship (CGS).

Received: October 8, 2010
Revised: January 7, 2011
Accepted: February 15, 2011
Published: April 21, 2011

REFERENCES

Barnouin, K., Leier, I., Jedlitschky, G., Pourtier-Manzanedo, A., Konig, J., Lehmann, W.D., and Keppler, D. (1998). Multidrug resistance protein-mediated transport of chlorambucil and melphalan conjugated to glutathione. Br. J. Cancer *77*, 201–209.

Begleiter, A., Mowat, M., Israels, L.G., and Johnston, J.B. (1996). Chlorambucil in chronic lymphocytic leukemia: mechanism of action. Leuk. Lymphoma *23*, 187–201.

Buick, R.N., Till, J.E., and McCulloch, E.A. (1977). Colony assay for proliferative blast cells circulating in myeloblastic leukaemia. Lancet *1*, 862–863.

Carreon, J.R., Stewart, K.M., Mahon, K.P., Jr., Shin, S., and Kelley, S.O. (2007). Cyanine dye conjugates as probes for live cell imaging. Bioorg. Med. Chem. Lett. *17*, 5182–5185.

Davis, S., Weiss, M.J., Wong, J.R., Lampidis, T.J., and Chen, L.B. (1985). Mitochondrial and plasma membrane potentials cause unusual accumulation

and retention of rhodamine 123 by human breast adenocarcinoma-derived MCF-7 cells. J. Biol. Chem. *260*, 13844–13850.

Fan, W., Richter, G., Cereseto, A., Beadling, C., and Smith, K.A. (1999). Cytokine response gene 6 induces p21 and regulates both cell growth and arrest. Oncogene *18*, 6573–6582.

Frezza, C., Cipolat, S., and Scorrano, L. (2007). Organelle isolation: functional mitochondria from mouse liver, muscle and cultured fibroblasts. Nat. Protoc. *2*, 287–295.

Hanahan, D., and Weinberg, R.A. (2000). The hallmarks of cancer. Cell *100*, 57–70.

Horton, K.L., and Kelley, S.O. (2009). Engineered apoptosis-inducing peptides with enhanced mitochondrial localization and potency. J. Med. Chem. *52*, 3293–3299.

Horton, J.K., Roy, G., Piper, J.T., Van Houten, B., Awasthi, Y.C., Mitra, S., Alaoui-Jamali, M.A., Boldogh, I., and Singhal, S.S. (1999). Characterization of a chlorambucil-resistant human ovarian carcinoma cell line overexpressing glutathione S-transferase mu. Biochem. Pharmacol. *58*, 693–702.

Horton, K.L., Stewart, K.M., Fonseca, S.B., Guo, Q., and Kelley, S.O. (2008). Mitochondria-penetrating peptides. Chem. Biol. *15*, 375–382.

Lakshmipathy, U., and Campbell, C. (1999). The human DNA ligase III gene encodes nuclear and mitochondrial proteins. Mol. Cell. Biol. *19*, 3869–3876.

Lowe, S.W., and Lin, A.W. (2000). Apoptosis in cancer. Carcinogenesis *21*, 485–495.

Lu, B., Yu, H., Chow, C., Li, B., Zheng, W., Davis, R.J., and Flavell, R.A. (2001). GADD45gamma mediates the activation of the p38 and JNK MAP kinase pathways and cytokine production in effector TH1 cells. Immunity *14*, 583–590.

Minn, A.J., Rudin, C.M., Boise, L.H., and Thompson, C.B. (1995). Expression of bcl-xL can confer a multidrug resistance phenotype. Blood *86*, 1903–1910.

Modica-Napolitano, J.S., and Aprille, J.R. (1987). Basis for the selective cytotoxicity of rhodamine 123. Cancer Res. *47*, 4361–4365.

Modica-Napolitano, J.S., and Aprille, J.R. (2001). Delocalized lipophilic cations selectively target the mitochondria of carcinoma cells. Adv. Drug Deliv. Rev. *49*, 63–70.

Modica-Napolitano, J.S., Koya, K., Weisberg, E., Brunelli, B.T., Li, Y., and Chen, L.B. (1996). Selective damage to carcinoma mitochondria by the rhodacyanine MKT-077. Cancer Res. *56*, 544–550.

Muratovska, A., Lightowlers, R.N., Taylor, R.W., Wilce, J.A., and Murphy, M.P. (2001). Targeting large molecules to mitochondria. Adv. Drug Deliv. Rev. *49*, 189–198.

Pepper, C., Thomas, A., Hoy, T., and Bentley, P. (1999). Chlorambucil resistance in B-cell chronic lymphocytic leukaemia is mediated through failed Bax induction and selection of high Bcl-2-expressing subclones. Br. J. Haematol. *104*, 581–588.

Reed, J.C. (1998). Bcl-2 family proteins. Oncogene *17*, 3225–3236.

Santos, J.H., Hunakova, L., Chen, Y., Bortner, C., and Van Houten, B. (2003). Cell sorting experiments link persistent mitochondrial DNA damage with loss of mitochondrial membrane potential and apoptotic cell death. J. Biol. Chem. *278*, 1728–1734.

Santos, J.H., Meyer, J.N., Mandavilli, B.S., and Van Houten, B. (2006). Quantitative PCR-based measurement of nuclear and mitochondrial DNA damage and repair in mammalian cells. Methods Mol. Biol. *314*, 183–199.

Smith, M.L., and Fornace, A.J., Jr. (1996). Mammalian DNA damage-inducible genes associated with growth arrest and apoptosis. Mutat. Res. *340*, 109–124.

Sunters, A., Springer, C.J., Bagshawe, K.D., Souhami, R.L., and Hartley, J.A. (1992). The cytotoxicity, DNA crosslinking ability and DNA sequence selectivity of the aniline mustards melphalan, chlorambucil and 4-[bis(2-chloroethyl) amino] benzoic acid. Biochem. Pharmacol. *44*, 59–64.

Taylor, R.C., Cullen, S.P., and Martin, S.J. (2008). Apoptosis: controlled demolition at the cellular level. Nat. Rev. Mol. Cell Biol. *9*, 231–241.

Thomas, J.J., Kim, J.H., and Mauro, D.M. (1992). 4-(4-nitrobenzyl)pyridine tests for alkylating agents following chemical oxidative activation. Arch. Environ. Contam. Toxicol. *22*, 219–227.

Yang, W.Z., Begleiter, A., Johnston, J.B., Israels, L.G., and Mowat, M.R. (1992). Role of glutathione and glutathione S-transferase in chlorambucil resistance. Mol. Pharmacol. *41*, 625–630.

Yousif, L.F., Stewart, K.M., Horton, K.L., and Kelley, S.O. (2009). Mitochondria-penetrating peptides: sequence effects and model cargo transport. ChemBioChem *10*, 2081–2088.